ISBN: 978-3-95450-233-2 ISSN: 2673-5504 doi:10.18429/JACoW-SRF2021-TUOFDV08

FIRST βNMR RESULTS ON SRF SAMPLES AT TRIUMF

E. Thoeng*[1], R.M.L. McFadden, P. Kolb, T. Junginger[2], Md. Asaduzzaman[2], R. E. Laxdal, V. L. Karner[3,4], D. Fujimoto[1,4], A. Chatzichristos[1†], J. O. Ticknor[3], J. R. Adelman[3‡], M. H. Dehn[1], C. D. P. Levy, R. Li, I. McKenzie, M. Stachura, S. R. Dunsiger[5], G. D. Morris, W. Andrew MacFarlane[3,4], R. F. Kiefl[1,4]
TRIUMF, Vancouver, BC, Canada
D. L. Cortie, ANSTO, Lucas Heights, NSW, Australia
[1]also at Department of Physics & Astronomy, University of British Columbia, Vancouver, BC, Canada
[2]also at Department of Physics & Astronomy, University of Victoria, Victoria, BC, Canada
[3]also at Department of Chemistry, University of British Columbia, Vancouver, BC, Canada
[4]also at Stewart Blusson Quantum Matter Institute, Vancouver, BC, Canada
[5] also at Department of Physics, Simon Fraser University, Burnaby, BC, Canada

Abstract

The βNMR (β-detected nuclear magnetic resonance) facility at TRIUMF offers the possibility of depth-resolved probing of the Meissner state over the first 100 nm below a sample surface. The measurement can give the attenuation of the applied magnetic field, as a function of depth. The technique can be especially important when probing layered systems like the dirty/clean S-S (superconductor-superconductor) bilayer and S-I-S (Superconductor-Insulator-Superconductor) structures. The TRIUMF SRF (Superconducting RF) group has recently completed first measurements at beta-NMR on Nb samples with various treatments. The results and method will be reported.

MOTIVATIONS FOR βNMR SRF STUDIES

Superconducting RF (SRF) cavity performance, characterized by the Q_0 (intrinsic quality factor) vs. E_{acc} (accelerating gradient) curve, is fundamentally limited by superconducting quench at high RF magnetic fields where the SRF cavity undergoes transition from the Meissner state to the highly dissipative vortex state. In the Meissner state, magnetic fields are screened within the so-called *London layer*, and therefore RF dissipation is contained only within a tens of nm from the inner SRF cavity surface. As the fields are increased, however, the surface barrier to magnetic flux penetration can be overcome and the magnetic flux penetrates into the bulk of the SRF cavities, which quenches the superconductivity due to high dissipation from rapidly oscillating flux vortices in the RF fields. In Niobium (Nb), the theoretical limiting RF magnetic field for an ideal surface is on the order of the superheating field, $\mu_0 H_{sh}$ ~240 mT at 0 K [1]. In the presence of surface defects, however, the limiting field is reduced towards the lower superconducting critical field, $\mu_0 H_{c1}$ (~174 mT at 0 K [2]).

In practice, the Q_0 vs. E_{acc} degrades at much lower fields due to a phenomenon called the *Q-slope*. The complete picture of the *Q-slope* is not yet fully understood but it is clearly related to the detailed material properties in the vicinity of the surface. Practical remedies have been developed in the form of low/medium temperature heat treatment (e.g., 120 °C bake which cures the *high-field Q-slope*). Various impurity doping recipes (e.g., nitrogen doping [3] and infusion [4]) have also been developed in the production of high-performance SRF cavities. A novel approach using thin film coating of higher H_c superconductors on Nb cavities for bilayer S-S (superconductor-superconductor) [5] and multilayer S-I-S (superconductor-insulator-supeconductor) [6] on Nb SRF cavities have also been proposed to further increase the limiting field beyond that of bulk Nb, as well as providing additional barriers to flux penetration at much higher fields.

Various surface studies of SRF cavity cut-outs and SRF Nb samples have elucidated the important role of the nm RF surface. The aforementioned heat treatment and impurity doping recipes have been shown to alter the impurity concentration profile near the surface, but a direct correlation on how they affect the Meissner state at high magnetic fields is not fully understood (though a detailed theoretical framework has been proposed [7]). An ideal characterization technique would allow for a direct measure of the magnetic field screening in the Meissner state in a the depth-resolved manner within the nm *London layer*, especially at high-parallel magnetic fields (fields parallel to the sample surface). The depth-resolved capabilities would allow a better understanding of how to engineer surface impurity concentrations via various heat-treatment/doping recipes in order to obtain custom SRF performance. The parallel magnetic field configuration is usually used to simulate the orientation of rf magnetic fields in SRF cavities.

A powerful technique to measure the local magnetic field is by implanting spin-polarized probes which interact with local electromagnetic fields inside a host material, wherein the local field is quantified by monitoring the time evolution of the probe's nuclear spin polarization. TRIUMF host two

* ethoeng@triumf.ca
† Current address: National Centre of Scientific Research "Demokritos", Agia Paraskevi, Greece
‡ Email: jradelman@berkeley.edu; Current address: Department of Chemistry, University of California, Berkeley, CA, USA

ISBN: 978-3-95450-233-2 ISSN: 2673-5504 doi:10.18429/JACoW-SRF2021-TUOFDV08

facilities for this purpose: one for muon spin resonance (μSR) facility and another for βNMR facility [8].

The muon beam at TRIUMF is delivered at relatively high energy and therefore is implanted deep into the bulk of Nb samples (150 µm, much deeper than the London layer). Depth-resolved surface and interface studies at TRIUMF can be done at the βNMR facility, which utilizes spin-polarized radioactive nuclei rather than the muon [9, 10]. The method is thus complimentary to the LE-μSR technique used at the Paul-Scherrer-Institute [11], but the latter is limited to parallel magnetic field parallel of 30 mT due to the strong deflection of the much lower magnetic rigidity of the low-energy muons.

To date, no facility is available to perform nm-scale depth-resolved local magnetic field measurements on SRF samples at high applied parallel fields. Delivering spin-polarized beam at higher fields is much easier using heavier ions, but requires a high-intensity radioactive (ion) beam facility such as the TRIUMF ISAC (Isotope Separator and Accelerator) facility [12]. This is the underlying motivation of developing the high-parallel-field spectrometer at TRIUMF βNMR facility.

OVERVIEW OF βNMR FACILITY

The principle of βNMR technique is to implant spin-polarized radioactive ion beam into samples, and to provide a measure of the local (magnetic) field by monitoring the time evolution of the probes' spin via its (asymmetric) β-decay [9, 10]. In order to achieve this, accelerated radioactive ion beam (such as the routinely used $^{8}Li^{+}$) are first produced and delivered by the TRIUMF ISAC accelerator complex [12], the beam is then spin-polarized using co-linear laser pumping scheme, capable of achieving up to ~70% spin polarization [13], and finally implanted into the sample.

The beam can be semi-simultaneously delivered to the two spectrometers, high-perpendicular-field (field perpendicular to sample surface) and the low-parallel-field (field parallel to sample surface) spectrometer as shown in Fig. 1 [9,10]. Only the parallel-field spectrometer, however, is suitable for the SRF studies. The low-parallel-field spectrometer is limited up to 24 mT. Currently, a high-parallel-field spectrometer has been installed by extending the existing low-parallel-field spectrometer beamline. The details are discussed in the later section of this paper.

The implantation energy of the beam is controlled via a high-voltage decelerator electrode mounted in front of the sample, thereby allowing low-energy implantation of the probes and a tunable implantation depth. This feature is essential in studying the magnetic field screening in the Meissner state of SRF samples. The magnetic field is applied parallel to the sample surface at the low-parallel-field spectrometer and therefore is suitable to simulate the magnetic field in SRF cavities.

The photo on the left of Fig. 2 shows the low-parallel-field spectrometer with the detector window removed. The directions of the beam, spin polarization, applied magnetic field, and detectors (plastic scintillators) configuration are shown in both the cross-section view and isometric view schematics at the top and bottom right of Fig. 2, respectively. This is the spectrometer used to obtain the first results of βNMR at low-field (up to 24 mT) in Nb SRF samples as further explained in the next section.

METHOD DEVELOPMENTS

Sample Preparation

Studies of SRF samples using muons have been done since 2010 at TRIUMF [14–16]. These studies resulted in the development of ellipsoid samples in order to measure the intrinsic field of the first vortex penetration in SRF samples undergoing different surface & heat treatments without geometric edge effect [17]. Annealing at 1400 °C has also been found to remove all pinning effects and is therefore used as a baseline for all the samples before undergoing further heat treatment / impurity doping [15]. Small Nb ellipsoids (measured at 10 mm× 4 mm on its major and minor axis, respectively) and custom sample holders have been prepared

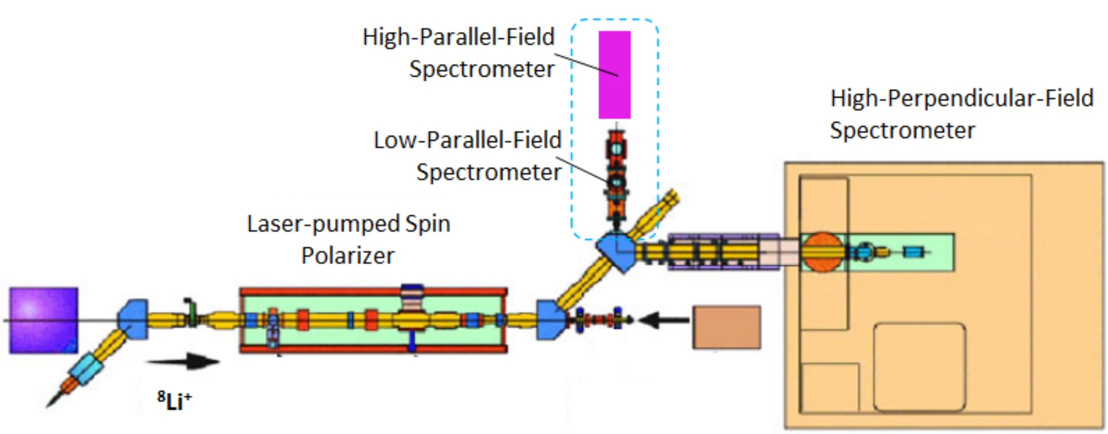

Figure 1: Schematics of the βNMR facility with radioactive beam delivered by TRIUMF ISAC facility. The spectrometer suited for the study of SRF samples are highlighted with the dashed box (adapted from [9]).

ISBN: 978-3-95450-233-2 ISSN: 2673-5504 doi:10.18429/JACoW-SRF2021-TUOFDV08

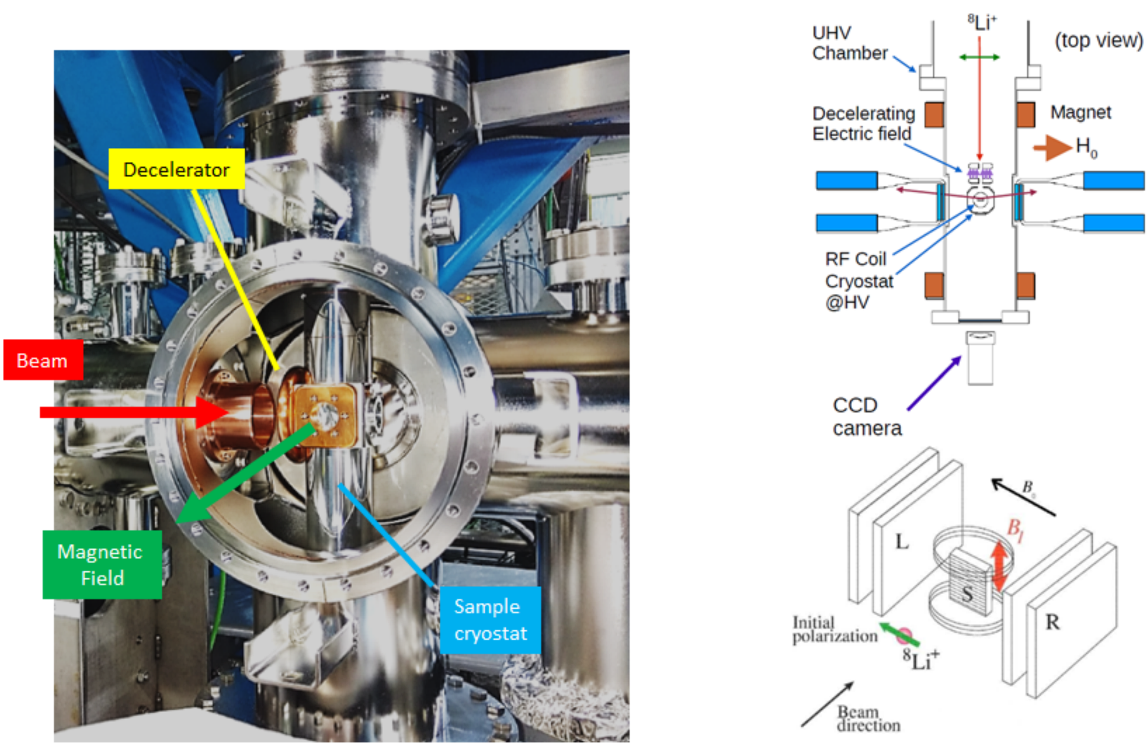

Figure 2: Left: Low-parallel-field spectrometer with detector and detector windows removed (courtesy of G.D.Morris). Right: Schematics of the beam momentum, spin polarization, magnetic field, and detectors configuration (adapted from [9]).

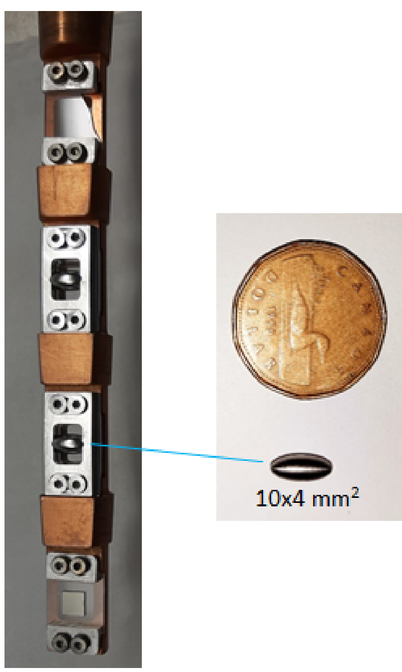

Figure 3: Sample ladder insert with two Nb SRF samples mounted on the second and third positions. Up to three samples can be mounted in a single load while one ladder spot is reseved for sapphire used to image and tune the beam position on sample. Shown in the right is the sample major and minor axes measured at ~10 mm and 4 mm, respectively, and its scale comparison with a Canadian *looney* (1$ coin).

to fit the sample ladder (shown in Fig. 3) which is inserted vertically into the cryostat via load-lock chamber.

Measurement Principles

In order to obtain the screened magnetic field profile, another important feature of this technique is the strong dependence of the spin-lattice relaxation rate with applied magnetic field. The relaxation rate is extracted from the fit of the asymmetry signal (shown in Fig. 4) using *bfit* package [18]. The sensitivity to local field is sensed primarily through the dipole-dipole coupling to the host ^{93}Nb nuclei with a phenomenological Lorentzian field dependence model of the relaxation rate. This method has been demonstrated in the measurement of London penetration depth in superconducting $NbSe_2$ [19] and is used for measurements in Nb SRF samples.

The radioactive beam (^{8}Li$^+$) is implanted into the sample and its spin polarization, observed via its beta-decay asymmetry, relaxes to a (thermal) equilibrium value in the sample (essentially zero). The rate of this relaxation depends on the time-averaged local magnetic field in the vicinity of the probe and therefore a measurement of the relaxation rate can be correlated with the measurement of the local magnetic field. This magnetic field sensitivity is demonstrated in Fig. 4 at 4 K near the surface where the field is of the same magnitude to the applied field with minimal Meissner screening.

A crucial component of obtaining the magnetic field profile is finding the relation between beam energy and the implantation profile. This relation can be predicted accurately with Monte-Carlo simulation of ^{8}Li$^+$ ions in Nb using SRIM code [20]. This method is similarly done for LE-μSR [11]. Smoothed implantation field profile is shown in Fig. 5 where

ISBN: 978-3-95450-233-2 ISSN: 2673-5504 doi:10.18429/JACoW-SRF2021-TUOFDV08

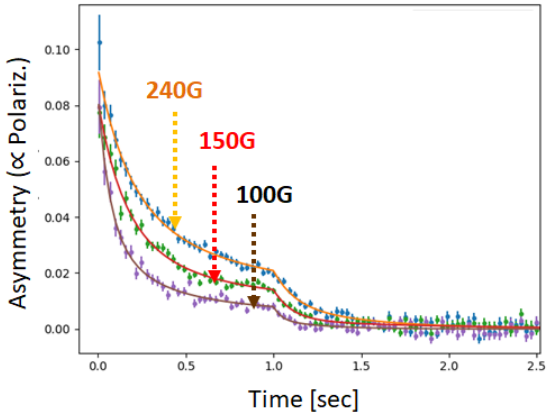

Figure 4: Relaxation of the asymmetry signal, proportional to the spin-polarization of the probes, is sensitive the local field at the probe implantation site. The pronounced kink is due to the 1 second beam pulse which is accounted for in the relaxation function fits shown. The measurement is performed at 4 K and 4 keV implantation energy. Shown here is the increase of the relaxation rate with decreasing applied fields.

at 20 keV, the range of the implanted $^{8}Li^{+}$ ions in Nb is ~150 nm, within the length scale of interest for SRF studies.

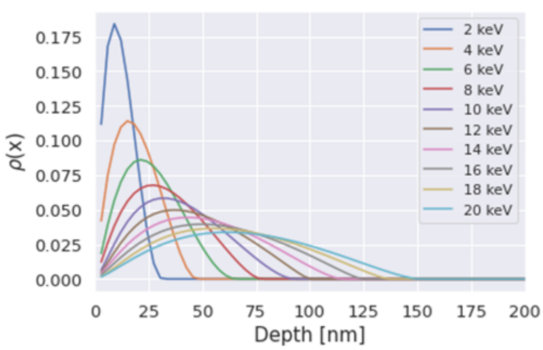

Figure 5: Implantation profiles obtained from Monte-Carlo simulation of $^{8}Li^{+}$ ions in Nb at different beam energies [20].

FIRST RESULTS ON SRF SAMPLES

Field Profile via Depth Scans

Using both the information of implantation profile and field dependent relaxation rate, the local field vs. mean depth can be obtained. Three samples: baseline Nb, 120 °C-baked Nb, and 75/120 °C two-step-baked Nb [21], have been extensively characterized and the result is summarized in Fig. 6. The field value is normalized to the value at the unscreened dead layer. The field profile shows less screening in 120 °C-baked Nb sample compared to the baseline Nb sample, consistent with the LE-μSR results in ref. [22]. The contrast between samples are limited by the low statistics of the fast relaxing polarization at low fields. To obtain better contrast, either measurements need to be done at higher fields to slow the relaxation rate, or different scans such as temperature scans (T-scans) are needed as described below.

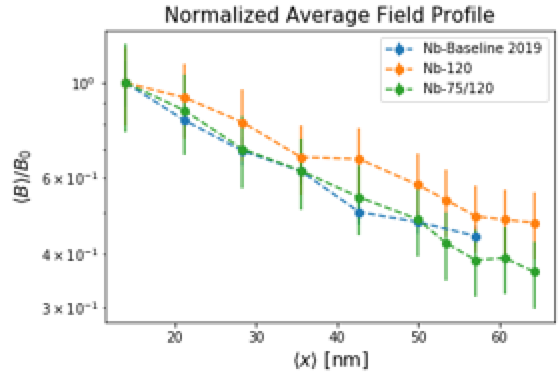

Figure 6: Field profile for three Nb SRF samples, normalized to their unscreened field value (i.e. applied field at sample surface considering the demagnetization factor) at the dead layer, which is estimated at ~15 nm.

Screening Profile via Temperature Scans

Relaxation rate are strongly enhanced as the temperature is decreased across T_c. This is due to the field expulsion from the bulk of the superconductor in the Meissner state which results to an abrupt increase in the relaxation rate below T_c. The stark contrast in the signal between measurements near the surface (with minimal Meissner screening) and in the bulk (with strong screening) can be clearly seen in Fig. 7, despite the fact that the measurements were performed at low applied field of only ~20 mT. For the case of 20 keV implantation energy, sputtered thin film Nb(300 nm)/Al_2O_3 is used as a control sample to illustrate the ideal trend for T-scan in flat and highly-oriented Nb [23]. Measurements of T-scans at different depth can therefore be used to characterize the screening profile of different samples with better resolution at low-field, as well as to self-consistently check the field profile obtained from the energy scans.

In order to illustrate the mutual dependence of the two independent variables in the measurement (temperature and implantation energy), the fit model extracted from T-scan at 20 keV is extrapolated and plotted as a 2D colour map shown in Fig. 8. The plot shows a clear contrast in colour, going from the normal to the superconducting state, as well as from shallow beam implantation in the dead layer with minimal screening compared to deeper implantation in the bulk with strong screening. Extensive amount of experimental shifts on the new high-parallel-field spectrometer (described in the next section) have been granted starting in August 2021 to map this parameter space for various heat-treated SRF samples.

HIGH-PARALLEL-FIELD βNMR SPECTROMETER

Upgrade Status

The high-parallel-field spectrometer consists of modified upstream existing beamline, extended new beamline (~1 m additional length), and high-field coil with fields up to 200 mT. Details on the beam optics and beam diagnostics,

ISBN: 978-3-95450-233-2 ISSN: 2673-5504 doi:10.18429/JACoW-SRF2021-TUOFDV08

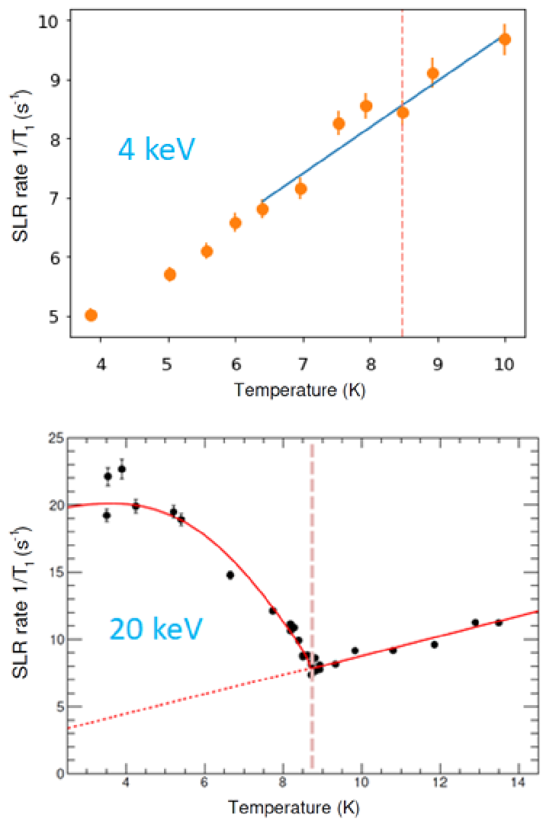

Figure 7: Temperature scans of relaxation rate in Nb SRF sample at 4 keV (top) and in Nb thin film sample at 20 keV (bottom) implantation energy. The vertical dash line indicates the transition temperature at anapplied field of 20 mT (~8.5 K). The sold lines are fits to a phenomenological model describing the temperature dependence and the screening in the Meissner state.

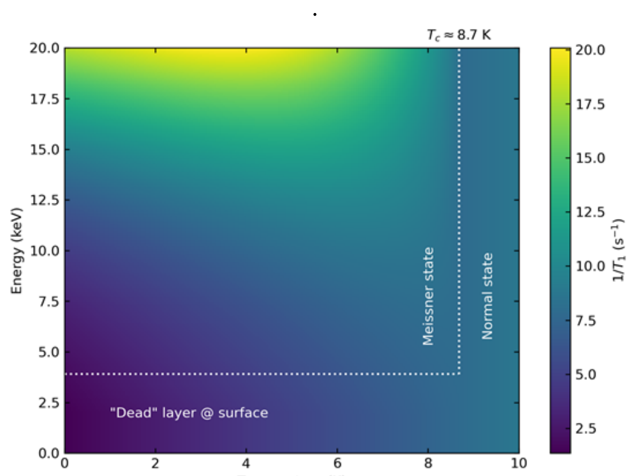

Figure 8: The depth-resolved T-scan plotted as 2D colour map to better show the contrast between dead and screened layer, and between normal ($T > T_c$) and Meissner state ($T < T_c$).

as well as the installation of the beamline have been reported on the previous proceeding of SRF2019 conference [24]. The schematics of the spectrometer is shown in Fig. 9 and the current state of the installed spectrometer is shown in the photo in Fig. 10. The high-parallel-field spectrometer is currently being prepared for its first experiment with radioactive beam scheduled in August 2021.

Future Studies with High-Parallel-Field Spectrometer

The high-parallel-field spectrometer allows exploration of additional parameter space, i.e. field scans up to 200 mT, in combination with nm depth resolution. Measurement at higher fields can provide better distinction between different SRF samples due to slower relaxation rate which corresponds to higher statistics for each sample. This new high-parallel-field capability also opens up pathway towards interesting studies of SRF material response at high magnetic field not available with other techniques. It is also of interest for the wider condensed matter community to have a tool to measure at high parallel magnetic field enabled by this spectrometer.

The depth-resolved measurement at high-fields can be used to correlate the impurity concentration profile (via heat treatment or impurity doping) with the screening response in a layer-by-layer manner. Therefore, each measurement acts as a unique *fingerprint* for various recipes, in a similar manner as the Q_0 vs. E_{acc} curves are used to catalogue different performance of SRF cavities. The main advantage is a detailed picture of why a certain treatment is giving improvements by measuring the flux screening in the London layer.

Continuing on previous field of first flux/vortex entry studies done at TRIUMF using μSR [15, 16, 25], the high-parallel-field spectrometer can provide crucial information on whether the higher fields of first flux entry in coated Nb samples are due to the additional S-S interface barrier as predicted in ref. [5], or due to other mechanisms, e.g. proximity effect as in ref. [25]. Depth resolved studies at high magnetic field can be used to monitor whether flux penetration are hindered at the S-S interface (while allowing flux penetration at the top dirty layer at ~ H_{c1}), or the penetration occurs immediately once the field at sample surface (H_{surface}) exceeds the superheating field (H_{sh}) regardless of the S-S interface. Similar studies can also be performed in S-I-S multilayer system to measure the layer-by-layer field profile and barrier to flux penetration in direct comparison with the theoretically predicted profile in ref. [6, 7].

CONCLUSION

The βNMR technique is a unique tool which can be used to probe the local magnetic field in SRF samples in a depth-resolved manner. Both the TRIUMF βNMR facility and spectrometers have been described in detail, and the first results in SRF samples using the low-parallel-field spectrometer have been presented. Temperature scans can be combined with depth-scans can enhance the contrast between samples when limited at low magnetic field and lower statistics. A high-parallel-field spectrometer has been built

ISBN: 978-3-95450-233-2 ISSN: 2673-5504 doi:10.18429/JACoW-SRF2021-TUOFDV08

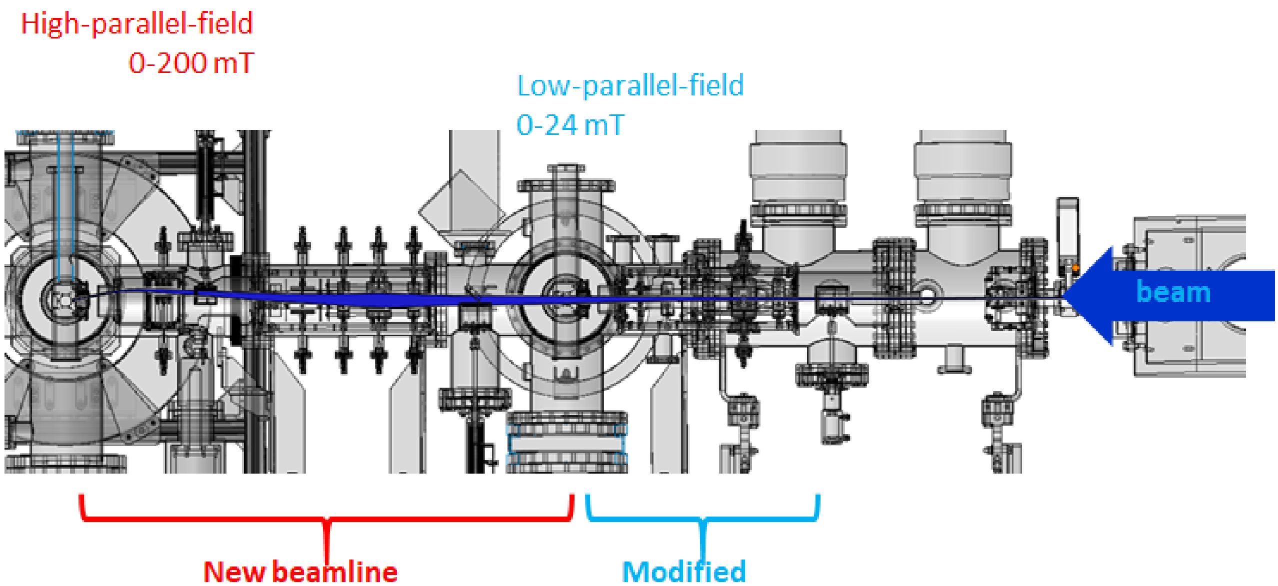

Figure 9: Cross-section view of the high-field spectrometer, the upstream beam optics, and low-parallel-field spectrometer. Also shown in the center of beamline axis is the beam deflection due to high-parallel magnetic field (courtesy of B. Matheson).

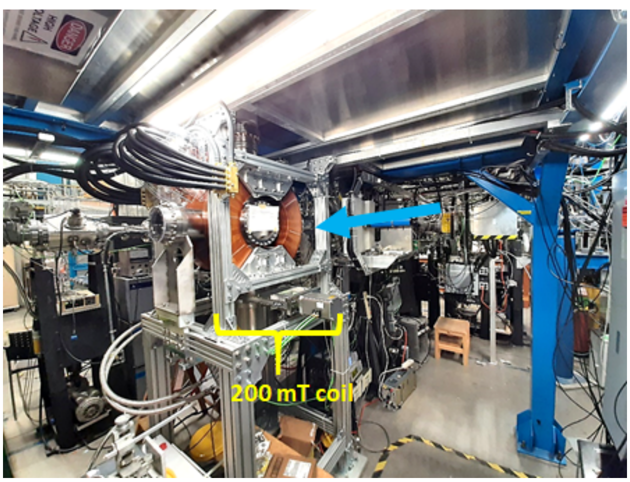

Figure 10: Latest photo of the installed high-parallel-field spectrometer. Shown in the photo is the high-parallel-field (200 mT) coil under the high-voltage platform used to decelerate the beam implantation energy at the sample. The blue arrow indicates the direction of the beam.

in order to allow depth-resolved study of SRF samples close to the H_{sh} of Nb. This facility will be unique in the world. The high-parallel-field spectrometer has been installed and is currently being prepared for its first experiment in August 2021.

ACKNOWLEDGEMENTS

This project is funded as a part of NSERC (Natural Science and Engineering Research Council) project grant. E. T. and A.C. acknowledge the support from NSERC IsoSiM Fellowship, and D.F. from a SBQMI QuEST Fellowship.

REFERENCES

[1] M. Transtrum, G. Catelani, and J. Sethna, "Superheating field of superconductors within Ginzburg-Landau theory", *Phys. Rev. B*, vol. 83, p. 094505, Mar. 2011. doi:10.1103/PhysRevB.83.094505

[2] D. Finnemore, T. Stromberg, and C. Swenson, "Superconducting Properties of High-Purity Niobium", *Phys. Rev.*, vol. 149, pp. 231–243, Sept. 1966. doi:10.1103/PhysRev.149.231

[3] A. Grassellino, A. Romanenko, D. Sergatskov, O. Melnychuk, Y. Trenikhina, A. Crawford, A. Rowe, M. Wong, T. Khabiboulline, and F. Barkov, "Nitrogen and argon doping of niobium for superconducting radio frequency cavities: a pathway to highly efficient accelerating structures", *Superconductor Science And Technology*, vol. 26, p. 102001, Aug. 2013. doi:10.1088/0953-2048/26/10/102001

[4] A. Grassellino, A. Romanenko, Y. Trenikhina, M. Checchin, M. Martinello, O. Melnychuk, S. Chandrasekaran, D. Sergatskov, S. Posen, A. Crawford, S. Aderhold, and D. Bice, "Unprecedented quality factors at accelerating gradients up to 45 MVm^{-1} in niobium superconducting resonators via low temperature nitrogen infusion", *Superconductor Science And Technology*. vol. 30, p. 094004, Aug. 2017. doi:10.1088/1361-6668/aa7afe

[5] T. Kubo, "Multilayer coating for higher accelerating fields in superconducting radio-frequency cavities: a review of theoretical aspects", *Superconductor Science And Technology*, vol. 30, p. 023001, Dec. 2016. doi:10.1088/1361-6668/30/2/023001

[6] A. Gurevich, "Maximum screening fields of superconducting multilayer structures", *AIP Advances*, vol. 5, p. 017112, 2015. doi:10.1063/1.4905711

[7] A. Gurevich, "Theory of RF superconductivity for resonant cavities", *Superconductor Science And Technology*, vol.

ISBN: 978-3-95450-233-2 ISSN: 2673-5504 doi:10.18429/JACoW-SRF2021-TUOFDV08

30, p. 034004, Jan. 2017. doi:10.1088/1361-6668/30/3/034004

[8] S. Kreitzman and G. Morris, “TRIUMF MuSR and βNMR Research Facilities”, in *Proc. of the 14th International Conference on Muon Spin Rotation, Relaxation and Resonance (μSR2017)*, Sapporo, Japan, Jun. 2017. p. 011056. doi:10.7566/JPSCP.21.011056

[9] G. D. Morris, “β-NMR”, in *ISAC and ARIEL: The TRIUMF Radioactive Beam Facilities and The Scientific Program*, J. Dilling and L. Merminga, Ed. Dordrecht, Netherlands: Springer, 2014, pp. 173-182. doi:10.1007/978-94-007-7963-1_19

[10] W. MacFarlane, “Implanted-ion βNMR: A new probe for nanoscience”, *Solid State Nuclear Magnetic Resonance*, vol. 68–69, pp. 1–12, Jun.–Jul. 2015. doi:10.1016/j.ssnmr.2015.02.004

[11] A. Simões, H. Alberto, R. Vilão, , J. Gil, J. Cunha, M. Curado, P. Salomé, .T. Prokscha, A. Suter, and Z. Salman, “Muon implantation experiments in films: Obtaining depth-resolved information”, *Review Of Scientific Instruments*, vol. 91, p. 023906, 2020. doi:10.1063/1.5126529

[12] J. Dilling and R. Krücken, “The experimental facilities at ISAC”, in *ISAC and ARIEL: The TRIUMF Radioactive Beam Facilities and The Scientific Program*, J. Dilling and L. Merminga, Ed. Dordrecht, Netherlands: Springer, 2014, pp. 111–114. doi:10.1007/978-94-007-7963-1_10

[13] C. D. P. Levy, M. R. Pearson, R. F. Kiefl, E. Manè, G. D. Morris, and A. Voss, “Laser Polarization Facility”, in *ISAC and ARIEL: The TRIUMF Radioactive Beam Facilities and The Scientific Program*, J. Dilling and L. Merminga, Ed. Dordrecht, Netherlands: Springer, 2014, pp. 165–172. doi:10.1007/978-94-007-7963-1_18

[14] A. Grassellino, C. Beard, P. Kolb, R. Laxdal, N. S. Lockyer, D. Longuevergne, and J. E. Sonier, “Muon spin rotation studies of niobium for superconducting rf applications”, *Phys. Rev. ST Accel. Beams*, vol. 16, p. 062002, Jun. 2013. doi:10.1103/PhysRevSTAB.16.062002

[15] T. Junginger, S. H. Abidi, R. D. Maffett, T. Buck, M. H. Dehn, S. Gheidi, R. Kiefl, P. Kolb, D. Storey, E. Thoeng, W. Wasserman, and R. E. Laxdal, “Field of first magnetic flux entry and pinning strength of superconductors for rf application measured with muon spin rotation”, *Phys. Rev. ST Accel. Beams*, vol. 21, p. 032002, Mar. 2018. doi:10.1103/PhysRevAccelBeams.21.032002

[16] T. Junginger and R. E. Laxdal, “Review of Muon Spin Rotation Studies of SRF Materials”, in *Proc. 19th Int. Conf. RF Superconductivity (SRF'19)*, Dresden, Germany, Jun.-Jul. 2019, pp. 360–363. doi:10.18429/JACoW-SRF2019-TUFUA7

[17] E. Brandt, “Superconductors in realistic geometries: geometric edge barrier versus pinning”, *Physica C: Superconductivity*. vol. 332, pp. 99–107, May 2000. doi:10.1016/S0921-4534(99)00651-6

[18] D. Fujimoto, “Digging Into MUD With Python: mudpy, bdata, and bfit”, [arXiv:2004.10395 [physics.data-an]].

[19] M. D. Hossain, Z. Salman, D. Wang, K. H. Chow, S. Kreitzman, T. A. Keeler, C. D. P. Levy, W. A. MacFarlane, R. I. Miller, G. D. Morris, T. J. Parolin, M. Pearson, H. Saadaoui, and R. F. Kiefl, “Low-field cross spin relaxation of ^{8}Li in superconducting $NbSe_2$”, *Phys. Rev. B.*, vol. 79, p. 144518, Apr. 2009. doi:10.1103/PhysRevB.79.144518

[20] J. Ziegler, M. Ziegler, and J. Biersack, “SRIM - The stopping and range of ions in matter (2010)”, *Nucl. Instr. Meth. in Phys. Research Sec. B*, vol. 268, pp. 1818–1823, Feb. 2010. 10.1016/j.nimb.2010.02.091

[21] A. Grassellino, A. Romanenko, D. Bice, O. Melnychuk, A. C. Crawford, S. Chandrasekaran, Z. Sung, D. A. Sergatskov, M. Checchin and S. Posen, *et al.* “Accelerating fields up to 49 MV/m in TESLA-shape superconducting RF niobium cavities via 75C vacuum bake”, [arXiv:1806.09824 [physics.acc-ph]].

[22] A. Romanenko, A. Grassellino, F. Barkov, A. Suter, Z. Salman, and T. Prokscha, “Strong Meissner screening change in superconducting radio frequency cavities due to mild baking”, *Applied Physics Letters*. vol. 104, p. 072601, 2014. doi:10.1063/1.4866013

[23] T. J. Parolin, J. Shi, Z. Salman, K. H. Chow, P. Dosanjh, H. Saadaoui, Q. Song, M. D. Hossain, R. F. Kiefl, C. D. P. Levy, M. R. Pearson, and W. A. MacFarlane, “Nuclear magnetic resonance study of Li implanted in a thin film of niobium”, *Phys. Rev. B*, vol. 80, p. 174109, Nov. 2009. doi:10.1103/PhysRevB.80.174109

[24] E. Thoeng *et al.*, “Progress of TRIUMF Beta-SRF Facility for Novel SRF Materials”, in *Proc. 19th Int. Conf. RF Superconductivity (SRF'19)*, Dresden, Germany, Jun.-Jul. 2019, pp. 964–967. doi:10.18429/JACoW-SRF2019-THP047

[25] T. Junginger, W. Wasserman, and R. E. Laxdal, “Superheating in coated niobium”, *Supercond. Sci. and Tech.* , vol. 30, p. 125012, Nov. 2017. doi:10.1088/1361-6668/aa8e3a